phys. stat. sol. (c) **5**, No. 1, 158–161 (2008) / **DOI** 10.1002/pssc.200776545

physica status solidi c
www.pss-c.com
*current topics in solid state physics*

# Few-particle electron dynamics in coupled quantum dots with phonon interaction

**Andrea Bertoni[1,*], Juan I. Climente[1], Massimo Rontani[1], Guido Goldoni[1,2], and Ulrich Hohenester[3]**

[1] National Research Center S3, INFM-CNR, Via Campi 213/A, 41100 Modena, Italy
[2] Dipartimento di Fisica, Università di Modena e Reggio Emilia, 41100 Modena, Italy
[3] Institut für Physik, Karl-Franzens-Universität Graz, Universitätsplatz 5, 8010 Graz, Austria

Received 9 July 2007, revised 7 August 2007, accepted 25 August 2007
Published online 11 October 2007

**PACS** 03.67.Lx, 72.10.Di, 73.21.La, 73.63.Kv

* Corresponding author: e-mail bertoni.andrea@unimore.it, Phone: +39-0592055295, Fax: +39-0592055616

The time evolution of a correlated multi-electron state in a semiconductor coupled quantum dot, interacting with the acoustic phonon bath, is calculated within the master equation formalism, including electron-electron interaction exactly through the configuration-interaction approach. The system is evolved after an initialization phase, with the system under strong bias, leading to the charge density mainly localized in one of the dots. When the system is evolved (in unbiased condition), damped multi-frequency charge oscillations are found, which strongly depend on the 3D system geometry and initialization. We describe the approach used to obtain the multi-electron states and to include the phonon-induced transitions between them in the time evolution. Furthermore, the effect of a magnetic field applied in the axial direction of the vertical double-dot cylindrical structure is discussed.

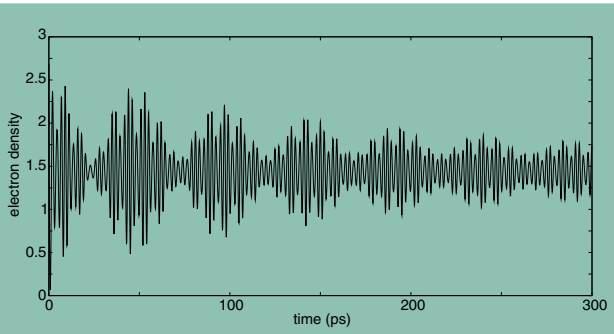


Evolution of the charge density (in units of the elementary charge) in one of the dots of a vertical double quantum dot with three electrons initially confined, by an electrical bias, in the same dot. The oscillation pattern shows multiple frequencies due to Coulomb correlation and is damped by the electron-phonon interaction. The frequencies are not damped uniformly and only one of them survives at long timescales.

© 2008 WILEY-VCH Verlag GmbH & Co. KGaA, Weinheim

**1 Introduction** Single-electron states in coupled quantum dots (CQDs) are ideal candidates for the realization of solid-state qubits [1–7]. Experiments able to detect the coherent oscillations of charge in such systems, have so far been performed in a multi-electron regime [8,9]. Quite surprisingly, a single-frequency oscillation has been revealed. It is thus of fundamental importance to properly model the dynamics of the multi-electron wave function in order to understand the conditions for a single-frequency oscillation and to map the time evolution of the multi-electron state on the time-evolution of the charge density (the quantity revealed in the experiments).

The physics of these oscillations is, in the single-particle case, well understood: when an electron is placed in one of the dots of a CQD system, with no other conduction-band electron in it, it oscillates back and forth between the dots with a frequency given by the energy difference between the bonding and antibonding states. This effect has analogues in coupled quantum wells and wires, where it has been measured [10–12] and proposed for some applications [13,14]. On the other hand, if more than one carrier is present in the CQD, the multi-particle Coulomb interaction plays an essential role in the dynamics of the oscillatory process and must be properly taken into account in the theoretical modeling of the system.

WILEY InterScience DISCOVER SOMETHING GREAT

© 2008 WILEY-VCH Verlag GmbH & Co. KGaA, Weinheim

The aim of the present work is to describe how the effect of Coulomb correlation can be included exactly in the calculation of the quantum dynamics of carriers in a CQD, with electron-phonon interaction. In the following Sec. 2 we describe the physical system and the procedure adopted to obtain the multi-particle states and their transition rates, then, in Sec. 3 we describe the initialization procedure and compute the coherent evolution of the multi-particle state, by also taking into account the effect of an external magnetic field. In Sec. 4 the effect of phonons is introduced and the result for the dissipative dynamics is discussed. Finally, in Sec. 5 we draw our conclusions.

**2 The multi-particle states and transitions** Our model system consists of a vertical GaAs/AlGaAs CQD, with disk shape and confinement energy in the range of few meV. The confinement potential is modeled as a double quantum well in the growth direction z, formed by the heterostructure band-offset, while, in the xy plane, a 2D parabolic confinement is assumed, which gives rise to the Fock-Darwin level structure [15]. The three-dimensional single-particle electronic states, computed within the envelope function approximation can be given the separable expression

$$\psi_{nmgs}(\mathbf{r},\sigma) = \phi_{nm}(x,y)\varphi_g(z)\chi_s(\sigma)\ , \qquad (1)$$

with $n$ and $m$ being the radial and angular quantum numbers of the Fock-Darwin state, respectively, $r$ the quantum number labeling the eigenfunction related to the double-well potential, and $s = \uparrow, \downarrow$ the spin state. The expression given in Eq. (1) for the single-particle states is valid also in the presence of a magnetic field $B$ in the vertical z direction. In the following, we will consider only the ground ($g = 0$) and first excited ($g = 1$) states of $\varphi_g(z)$, namely the bounding and antibounding state, respectively. In fact, in the structures under study, both the tunneling energy and the harmonic oscillator energy splitting $\hbar\omega_0$ are of the order of 1 meV, much lower than the energy gap between the first and the second excited states in the $z$ direction.

In order to expose the role of electronic correlations in the dynamics, we need a large number of multi-particle eigenstates with comparable precision. Our method of choice is a full configuration interaction procedure [16], that we briefly describe in the following. So far, the dynamics of two electrons in CQDs has been addressed using specific approximations for the Coulomb interaction, ranging from Hubbard models [5, 17] to configuration interactions with truncated basis sets. We stress that the CQD few-electron dynamics is distinct from previous findings in coupled quantum wells, where plasmon oscillations take place [11].

In the full configuration-interaction approach, each N-electron state $|\Psi_l\rangle$ is expressed in terms of a linear combination of Slater determinants $|\Psi_l\rangle = \sum_j c_{lj}|\Phi_j\rangle$. The Slater determinants $|\Phi_j\rangle$ are composed by populating the single-particle spin-orbitals $\psi_{nmgs}(\mathbf{r},\sigma)$ with N electrons in all possible ways, consistent with symmetry requirements. In order to obtain the coefficients $c_{lj}$, the Hamiltonian containing the Coulomb interaction is numerically diagonalized, exploiting orbital and spin symmetries [18].

Once the correlated states have been obtained, we compute the transition rates due to phonon scatterings by using the Fermi golden rule [19]. Expanding the correlated states on the Slater determinants, we obtain, for the transition from $|\Psi_b\rangle$ to $|\Psi_a\rangle$,

$$\gamma_{b\to a} = \frac{2\pi}{\hbar}\sum_{\mathbf{q}}\left|\sum_{ij} c^*_{bi}c_{aj}\langle\Phi_i|V_{\mathbf{q}}|\Phi_j\rangle\right|^2 \delta(E_b - E_a + \hbar\omega_{\mathbf{q}}), \qquad (2)$$

where $V_{\mathbf{q}}$ is the interaction operator of an electron with an acoustic phonon of momentum $\mathbf{q}$ via deformation potential and piezoelectric field interactions [20], $E_a$ stands for the energy of the N-electron state $|\Psi_a\rangle$, and $\hbar\omega_{\mathbf{q}}$ represents the phonon energy. From Eq. (2), it is clear that the transition rate $\gamma_{b\to a}$, between two correlated states, can be expressed in terms of a large number of transition amplitudes between the single-particle states that constitutes the Slater determinants $|\Phi_i\rangle$: $\langle\psi_{nmgs}|V_{\mathbf{q}}|\psi_{nmgs}\rangle$. The latter values are easily computed by a 3D real-space integration.

In the following computation of the time evolution we will need to overlap two N-particle wave functions obtained with different CQD potentials, namely without and with an external linear electrical bias $E_z$ applied along the z direction (used to initialize the system). To this aim it is useful to introduce a specific notation: an $E_z$ superscript will indicate a (single- or multi-particle) state of the biased system, with the lower dot at a lower potential energy. For the z component of the single-particle wave functions it holds $\varphi_0^{E_z}(z) = [\varphi_0(z) + \varphi_1(z)]/\sqrt{2}$ and $\varphi_1^{E_z}(z) = [\varphi_0(z) - \varphi_1(z)]/\sqrt{2}$, where the ground $\varphi_0^{E_z}$ and first excited $\varphi_1^{E_z}$ z states are localized in the lower and upper dot, respectively. The validity of the above conditions has been checked numerically for all the systems and initialization biases used in the following simulations.

**3 Coherent evolution** In this section we simulate the coherent evolution of the CQD electrons. As a first step we compute the ground N-particle state $|\Psi_0^{E_z}\rangle$ when a bias $E_z$ is applied, which localizes the electrons in the lower dot. This will be our initial condition. The number of particles effectively localized in the lower dot depends on the strength of the bias, that contrasts the Coulomb repulsion which would distribute the particles equally between the two dots.

As a second step we compute the N-particle eigenstates of the unbiased system (we suppose that the bias has been *non adiabatically* removed at time $t = 0$) and use them as a basis to evolve the correlated state

$$|\Psi^{E_z}(t)\rangle = \sum_l e^{-\frac{i}{\hbar}E_l t}\langle\Psi_l|\Psi_0^{E_z}\rangle|\Psi_l\rangle, \qquad (3)$$


© 2008 WILEY-VCH Verlag GmbH & Co. KGaA, Weinheim

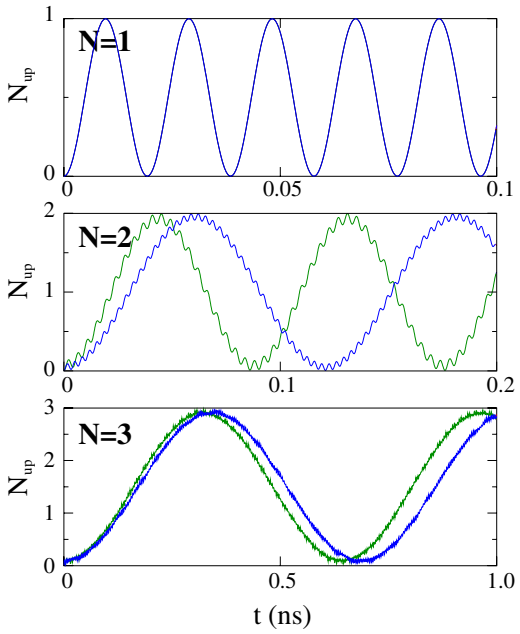


**Figure 1** Time evolution of the charge density (in units of elementary charge) in the upper dot of a vertical CQD with $N = 1$, 2 and 3 electrons. The system is initialized by an electrical bias $E_z = 200$ kV/m that localizes the carriers in the lower dot. The bias is removed at $t = 0$ and the N particles evolve coherently. The dots have vertical dimension of 10 nm, a parabolic in-plane confinement with energy spacings of 3 meV, and are coupled by a tunneling barrier 8 nm wide. The axial magnetic field is $B = 0$ for the darker/blue curve and $B = 5$ T for the lighter/green curve. Note the different scales used in the panels.

where $E_l$ is the energy of the $l$-th unbiased state. Note that the quantum states of Eq. (3) are multi-particle states and the computation of the coefficients $\langle \Psi_l | \Psi_0^{E_z} \rangle$ requires their expansion in terms of Slater determinants

$$\langle \Psi_l | \Psi_0^{E_z} \rangle = \sum_{jj'} c_{lj}^* c_j^{E_z} \langle \Phi_j | \Phi_{j'}^{E_z} \rangle. \qquad (4)$$

In order to represent the time evolution of the N-particle state, we report, in Fig. 1, the occupation of the upper dot (in units of number of particles) against the time. The cases with one, two and three electrons are shown, without and with an axial magnetic field (see caption). The initialization bias $E_z$ of 200 kV/m is able, in all the cases presented, to localize all the electrons in the lower dot. As a consequence all the graphs indicate, at time $t = 0$, an empty upper dot. As expected, the time evolution of the density is a sinusoidal oscillation for the single-electron case. Note that the curve obtained with the magnetic field matches exactly (thus, in the figure, cannot be distinguished form) the one without magnetic field. This can be easily understood by recalling that the single-particle wave function of Eq. (1) is separable in the xy and z components also when $B \neq 0$. The magnetic field, applied in the z direction, changes the

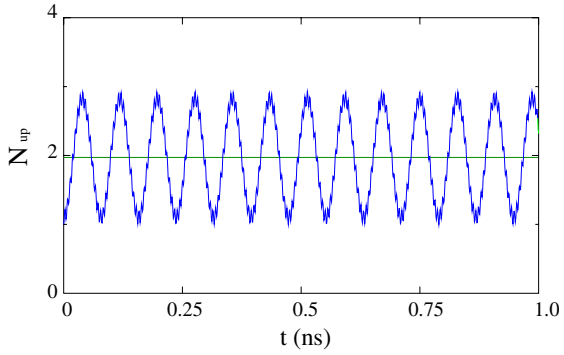


**Figure 2** Same as Fig. 1, with $B = 0$, for a CQD with four electrons. Two values of the initialization biases are shown: the stronger one $E_z = 100$ kV/m is able to partially contrast the Coulomb repulsion and localizes three electrons in the lower dot, while the weaker one $E_z = 75$ kV/m leaves two carriers in each dot. The latter does not produce visible time variations of the charge density (flat line at $N_{up} = 2$).

in-plane component $\phi_{nm}(x, y)$ of the wave function but it does not modify the $\varphi_g(z)$, which is responsible of the oscillation. In other words, an orthogonal magnetic field does not alter the tunneling energy and, as a consequence, the oscillation period.

When more electrons are present in the CQD, Coulomb interaction mixes the vertical and in-plane degrees of freedom so that a vertical magnetic field is able to tailor the oscillation period of the multi-particle wave function. This can be seen from the middle ($N = 2$) and bottom ($N = 3$) panels of Fig. 1. In general, the oscillation frequency increases with $B$, until its value become high enough to change the dominant Slater determinant of the ground state, in which case the oscillation pattern changes significantly. Another interesting, and quite unexpected, result shown by Fig. 1 is the evidence of a highly dominating frequency in the multi-particle CQD dynamics. In fact, we find that Coulomb correlation enhances only one of the frequencies related to the different single-particle vertical components of the N-particle states, as explained elsewhere [21]. A multi frequency dynamics can be obtained by reducing the effects of correlation with an artificial screening of the Coulomb potential or with a proper design of the CQD device (e.g. with a strong in-plane confinement) [21].

In Fig. 2 we report, as an example, the time-dependent occupancy of the top dot for a four-electron CQD system, without magnetic field, for two different values of the initialization bias. When the bias is small, it is not able to contrast the Coulomb repulsion, which, as stated before, tends to equally distribute the electrons between the dots. The system remains in its initial state, with two electrons in each dot. For a higher value of the bias, three electrons are initially localized in the bottom dot and one in the top, this leading to the oscillatory dynamics similar to that presented in Fig. 1, but with an amplitude of two particles. Also in this case, high-frequency modulations are super-

© 2008 WILEY-VCH Verlag GmbH & Co. KGaA, Weinheim 

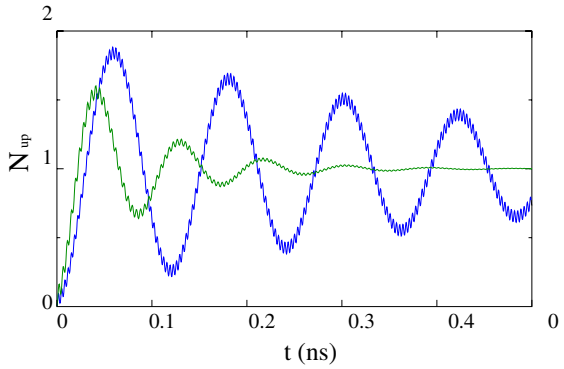


**Figure 3** Upper dot occupancy of the same CQD sample of Fig. 1, with two correlated electrons interacting with the phonon field. The two curves represent the case with $B = 0$ (darker/blue curve) and $B = 5$ T (lighter/green curve).

imposed to the dominant oscillation, coming from the different energies of the single-particle $\varphi_g(z)$ components of the multi-particle state.

**4 Dissipative evolution** In this Section we include the effects of phonons on the CQD evolution by using the transition rates between N-electron states obtained in Sect. 2. We account for three electron-acoustic phonons interaction mechanisms (the energy of the optical phonons is well above the energy of the electronic transitions considered), namely scattering due to the deformation potential, scattering from longitudinal piezoelectric field and scattering from transverse piezoelectric field. We simulate the system evolution by solving the Pauli master equation of the carrier states directly on the few-particle basis

$$\frac{d\rho_{ij}}{dt} = \frac{i}{\hbar}(E_j - E_i)\rho_{ij} - \sum_l \frac{\gamma_{j\to l} + \gamma_{i\to l}}{2}\rho_{ij} + \delta_{ij}\sum_l \gamma_{i\to l}\rho_{ll}, \quad (5)$$

where $\rho_{ij} = \langle\Psi_i|\hat{\rho}|\Psi_j\rangle$ is an element of the density matrix of the N-particle system, and the transition rates $\gamma_{i\to j}$ are given by Eq. (2).

We solve Eq. 5 by a direct diagonalization of the corresponding evolution operator $\breve{\mathcal{L}}$ defined by $\frac{d\hat{\rho}}{dt} = -\frac{i}{\hbar}\breve{\mathcal{L}}\hat{\rho}$. The resulting time dependence of the top dot occupancy is shown in Fig. 3 for a CQD with two interacting electrons, without and with an axial magnetic field. Here the oscillations are damped by the dissipation due to the interaction with the phonons. This effect is also apparent from the figure in the abstract, where a different sample is shown. While in the latter figure the different oscillation periods are of comparable amplitude and create beatings, in Fig. 3 one of the frequencies is dominant. The presence of the magnetic field, not only increases the oscillation frequency, as shown in the previous section, but also enhances the transition rates [20], and thus the damping.

**5 Conclusions** By using a configuration-interaction approach to account for Coulomb correlation effects, and a master equation approach for the effects of phonon interaction, we computed the time-evolution of the N-particle wave function in a vertical CQD. We found that the oscillatory pattern strongly depends on the geometry of the sample, and can range from a semi-chaotic multi-frequency one to a quasi single-frequency one, typical of the single-particle dynamics. The inclusion of an axial magnetic field generally reduces the oscillation frequency and, through its effect on the multi-particle transition rates, can increase the damping of the charge oscillations.

**Acknowledgements** We are grateful to Elisa Molinari and Filippo Troiani for helpful discussions. This work has been patially supported by FIRB-MIUR projects RBIN04EY74 and RBIN06JB4C and by Cineca-INFM Calcolo Parallelo 2007.

## References

[1] W. G. van der Wiel, M. Stopa, T. Kodera, T. Hatano, and S. Tarucha New J. Phys. **8**, 28 (2006).
[2] L. Fedichkin, M. Yanchenko, and K. A. Valiev, Nanotechnology **11**, 387 (2000).
[3] T. Tanamoto, Phys. Rev. A **61**, 22305 (2000).
[4] W. G. van der Wiel, T. Fujisawa, S. Tarucha, and L. P. Kouwenhoven, Jpn. J. Appl. Phys. **40**, 2100 (2001).
[5] T. Brandes and T. Vorrath, Phys. Rev. B **66**, 075341 (2002).
[6] S. Gardelis, C. G. Smith, J. Cooper, D. A. Ritchie, E. H. Linfield, Y. Jin, and M. Pepper, Phys. Rev. B **67**, 73302 (2003).
[7] U. Hohenester, Phys. Rev. B **74**, 161307(R) (2006).
[8] T. Hayashi, T. Fujisawa, H. D. Cheong, Y. H. Jeong, and Y. Hirayama, Phys. Rev. Lett. **91**, 226804 (2003); T. Fujisawa, T. Hayashi, H. D. Cheong, Y. H. Jeong, and Y. Hirayama, Physica E **21**, 1046 (2004).
[9] J. Gorman, D. G. Hasko, and D. A. Williams, Phys. Rev. Lett. **95**, 090502 (2005).
[10] A. Pashkin, T. Yamamoto, O. Astafiev, Y. Nakamura, D. V. Averin, and J. S. Tsai, Nature **421**, 823 (2003).
[11] K. Leo, J. Shah, E. O. Gobel, T. C. Damen, S. Schmitt-Rink, W. Schafer, and K. Kohler, Phys. Rev. Lett. **66**, 201 (1991).
[12] A. Ramamoorthy, J. P. Bird, and J. L. Reno, Appl. Phys. Lett. **89**, 13118 (2006).
[13] B. Laikhtman and L. D. Shvartsman, Phys. Rev. B **72**, 245333 (2005).
[14] A. Bertoni, P. Bordone, R. Brunetti, C. Jacoboni, and S. Reggiani, Phys. Rev. Lett. **84**, 5912 (2000).
[15] L. Jacak, P. Hawrylak, and A. Wojs, Quantum Dots (Springer Verlag, Berlin, 1998).
[16] M. Rontani, C. Cavazzoni, D. Bellucci, and G. Goldoni, J. Chem. Phys. **124**, 124102 (2006).
[17] C. E. Creffield and G. Platero, Phys. Rev. B **65**, 113304 (2001).
[18] J. I. Climente, A. Bertoni, M. Rontani, G. Goldoni, and E. Molinari, Phys. Rev. B **74**, 125303 (2006).
[19] A. Bertoni, M. Rontani, G. Goldoni, and E. Molinari, Phys. Rev. Lett. **95**, 066806 (2005).
[20] J. I. Climente, A. Bertoni, M. Rontani, G. Goldoni, and E. Molinari, Phys. Rev. B **74**, 35313 (2006).
[21] A. Bertoni, J. I. Climente, M. Rontani, G. Goldoni, and U. Hohenester, in preparation (2007).


© 2008 WILEY-VCH Verlag GmbH & Co. KGaA, Weinheim